

90-594



сообщения
Объединенного
института
ядерных
исследований
Дубна

E13-90-594

L.M.Soroko

LONGITUDINAL INTERFERENCE
OF THE DIFFRACTION FREE WAVE FIELDS.
III. APPLICATIONS

1990

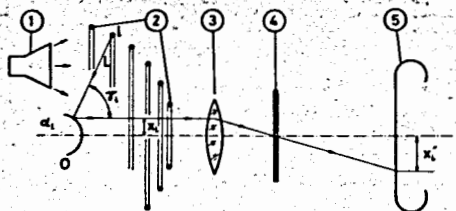


Fig. 1. The principle scheme of the traditional optical keratometer: 1 - illuminating system, 2 - coaxial mark rings, 3 - objective, 4 - aperture diaphragm, 5 - photocamera.

stage the coordinate mark 2 is illuminated by the system 1 and the image of these rings

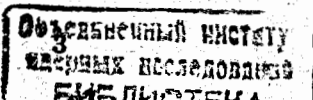
on the surface of the eye is registered by the photocamera 5 in the condition when the aperture diaphragm 4 transmits only the rays of the light which are parallel to the optical axis of the system. Owing to this the image of coordinate rings 2 consists of partially distorted circles. This initial information must be processed in the reconstructed stage. The operator estimates the radii R_i of the rings and then calculates the curvature radius of the rings on the eye for different distances from the optical axis. In the improvement versions of the traditional optical keratometer^{4, 5} the eye is illuminated by the collimated beams of light.

As was shown in⁶, the main source of the measurement errors in the traditional optical keratometers is the uncertainty of the longitudinal adjustment which introduces the error $\Delta R = 19 \mu\text{m}$ for the longitudinal shift $\Delta = 0.5 \text{ mm}$, $L = 200 \text{ mm}$ and $R = 8 \text{ mm}$. This sensitivity of the end results to the longitudinal disalignment is the first drawback of the traditional optical keratometer. The second drawback is of the pure mathematical nature. The operator must process the initial data by solving the inverse problem. Thus the measurements accomplished by the traditional optical keratometer are not direct ones and need the reconstruction stage.

3. CONFOCAL MESOPTICAL KERATOMETER

This new keratometer is named as a "meso-optical one" as it generates conical wave fronts in the illuminating system. For this purpose we use mirrors with generators in the form of the eccentric parabola. The meso-optical keratometer generates the sharp beam of light with longitudinal modulation of the light intensity along the optical axis of the device. The objective of the meso-optical keratometer sees only that part of the eye which is on the optical axis of the system, thus this meso-optical keratometer is a confocal device^{7, 8, 9}.

The principle construction of the confocal meso-optical keratometer is given in Fig. 2: 1 - point light source, 2 - concave



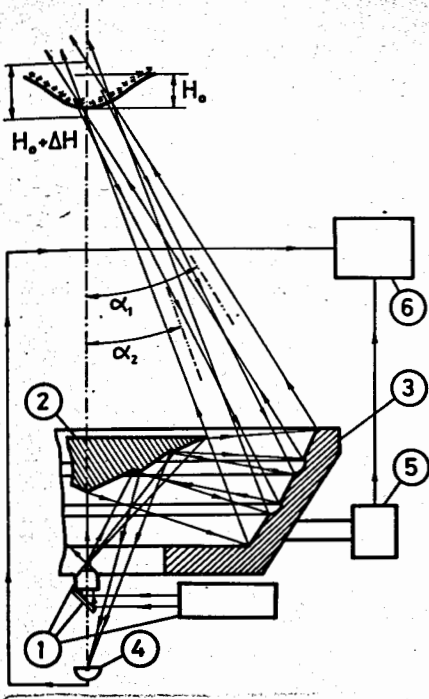


Fig. 2. The principle scheme of the confocal meso-optical keratometer: 1 - point light source, 2 - concave three element conical mirror, 3 - convex three element meso-optical mirror, 4 - point photodetector, 5 - the system of the transverse linear movement of the keratometer and the position encoder, 6 - computer memory block.

three-element mirror, 3 - convex three-element meso-optical mirror, 4 - point photodetector, 5 - the system of the transverse movement of the keratometer and the position encoder, and 6 - computer memory block. The mirrors 2 and 3 are a single block. The generator of the mirror 2 consists of three straight line segments, and the generator of the mirror 3 consists of three segments of the eccentric parabolas.

The external and internal segments of the generator of the conical mirror 2 are lying on the common straight line. The central segment of this generator is oriented with respect to this common straight line at the angle ϕ which must be chosen in accordance with eq. (1):

$$\phi = \arcsin \left[\frac{r_2}{L_1 + L_2 + r_2 \cos \gamma} \right] - \arcsin \left[\frac{r_2}{L_1 + r_2 \cos \gamma} \right], \quad (1)$$

where r_2 is the distance from the central segment of the generator of the mirror 2 to the optical axis of the keratometer, 2γ is the vertex angle of the conical mirror 2, L_1 is the distance from the vertex of the conical mirror 2 to the point light source 1, and L_2 is the distance from the point light source 1 to the point photodetector 4.

The external part of the generator of the meso-optical mirror 3 is the segment of the first eccentric parabola with focus in the point where the imaginary image of the light source 1 is formed by the mirror 2 and with axis parallel to the central ray going from the external part of the generator of the

mirror to the eye. The internal part of the generator of the meso-optical mirror 3 is the segment of the second eccentric parabola with focus in the point where the imaginary image of the light source 1 is formed by the mirror 2, and with axis parallel to the central ray going from the internal part of the generator of the meso-optical mirror 3 to the eye. The central part of the generator of the meso-optical mirror 3 is the segment of the third eccentric parabola with focus in the point where the imaginary image of the point photodetector 4 is formed by the mirror 2 and with axis parallel to the central ray going from the illuminated part of the eye to the central part of the generator of the meso-optical mirror 3.

The function of the illuminating part of this confocal meso-optical keratometer accomplish the external parts of the mirror 2 and of the meso-optical mirror 3. The function of the objective accomplish the internal parts of these mirrors.

Two coaxial wave fronts produce the longitudinal modulation of the light intensity on the optical axis of the device. This picture is shown in Fig. 3 where one of the meridional cross sections of the volume near the eye is presented. If the eye surface lying on the optical axis of the system is in the position where the light intensity is maximal, the reflected light will move to the central part of the meso-optical mirror 3, then to the central part of the mirror 2 and finally it will be picked up by the point photodetector 4. The photocurrent signal of the point photodetector 4 and the data from the position encoder 5 are fed into the computer memory block 6. If the eye surface on the optical axis of the system is in the position with zero light intensity then no reflected

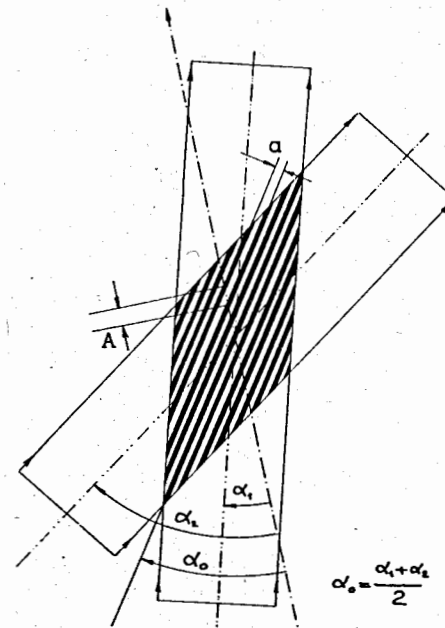


Fig. 3. The longitudinal interference of two coaxial conical wave fronts going at the angles α_1 and α_2 to the optical axis of the system, "a" is the period of the interference fringes and "A" is the period of the longitudinal interference.

light is generated and no photocurrent signal will go from the point photodetector 4.

The period A of the longitudinal modulation of the light intensity on the optical axis of the confocal meso-optical keratometer is given by the equation

$$A = \frac{\lambda}{\sin(\alpha_2 - \alpha_1) \sin\left(\frac{\alpha_1 + \alpha_2}{2}\right)}, \quad (2)$$

where λ is the wave length, α_2 and α_1 are the angles between the central rays going from the external and from the internal parts of the generator of the meso-optical mirror 3, respectively, and the optical axis of the system. For $\lambda = 0.5 \mu\text{m}$, $\alpha_2 = 35^\circ$, $\alpha_1 = 15^\circ$ we have $A = 3.5 \mu\text{m}$. For $\alpha_2 = 30^\circ$, $\alpha_1 = 20^\circ$ we have $A = 7 \mu\text{m}$. The period A of the longitudinal modulation of the light intensity which defines the errors of the measurement in the confocal meso-optical keratometer can be made smaller than $10 \mu\text{m}$.

As the objective of the whole system sees only the points which are lying on the optical axis of the system the device is indeed a confocal one^{8,9}. The point spread function of the confocal meso-optical keratometer in the plane perpendicular to the optical axis of the system is equal to:

$$I_2(\rho) = \text{Const.} |J_0(\alpha\rho)|^4, \quad (3)$$

where $\alpha\rho$ is the normalized distance from the optical axis of the confocal meso-optical keratometer to the observation point, and $J_0(\bullet)$ is the Bessel function of the zero order of the first kind. The intensity of the first side lobe in each half of our system is equal to 0.13 of the central maximum. The intensity of the first side lobe of the whole system is 0.016 of the central maximum. Owing to this property the confocal meso-optical keratometer offers very high noise immunity, as this device does not see practically that parts of the eye surface which are not on the optical axis of the device. The confocal meso-optical keratometer sees the objects inside the microscopic tube on the optical axis of the device, and the diameter of this microscopic tube is equal to

$$d = \frac{\lambda}{\sin\alpha_0}, \quad (4)$$

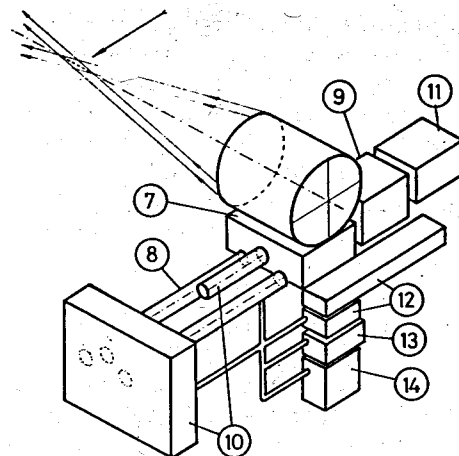


Fig.4. The whole assembly of the confocal meso-optical keratometer: 7 - moving stage, 8 - slabs of the moving stage, 9 - spring mechanism, 10 - air brake, 11 - trigger, 12 - diffraction gratings, 13 - illuminating block, 14 - electronics.

where $\alpha_0 = \frac{1}{2}(\alpha_1 + \alpha_2)$. For $\lambda = 0.5 \mu\text{m}$, $\alpha_2 = 30^\circ$, $\alpha_1 = 20^\circ$, we have $d \approx 1 \mu\text{m}$.

The whole assembly of the confocal meso-optical keratometer is shown in Fig.4. It comprises the following parts: 7 - the moving stage, 8 - the directing slabs of the moving stage, 9 - the spring, 10 - the illuminator and 14 - electronics.

The meso-optical part of this device moves in the direction perpendicular to the optical axis of the device as shown by the arrow on Fig.4. The surface of the eye is illuminated point by point along the chosen direction. The intermediate data in the computer memory block 6 consist of the moment of time t_i , where the photosignal assumes the maximal values, and of the moment of time τ_i when the device is in the points with increment step equal to $2.5 \mu\text{m}$. Thus we have in the memory of the computer the coordinates of this position mark. The nonuniformity of the movement of the moving part of the device does not have any influence on the measurement errors.

The time increment $\Delta t_i = t_{i+1} - t_i$ between the adjacent moments of time t_i is defined by the inclination angle of the tangent to the profile of the eye. When this tangent is parallel to the movement vector the time increment Δt_i is maximal. In this device the eye profile is sampling by means of the two dimensional coordinate grid with spacings equal to $2.5 \mu\text{m}$ along the movement axis, and equal to $5 \mu\text{m}$ along the optical axis of the device. Over the eye profile with depth 10 mm and length 10 mm the number of nodal points of this grid is equal to $2 \cdot 10^3 \cdot 10^3 = 8 \cdot 10^6$, which is three orders of magnitude greater than in the traditional optical keratometer, namely, $15 \cdot 15 \cdot 10^2 = 7.5 \cdot 10^3$.

With clock frequency of the device $f_0 = 0.4 \text{ MHz}$ we can sample $4 \cdot 10^2$ photopulses in the time interval 10^{-2} s , which corresponds to the movement velocity 1 m/s . The clock frequen-

cy $f_0 = 0.4$ MHz which defines the productivity of the device on the reading stage can be transformed into the audiofrequency $\nu_0 = 10^3$ Hz on the reproduction stage. The signals with this frequency can be reproduced by the magnetophone. The operator can "hear" the eye profile as a melody which at the beginning has a high tone, then low tone and to the end a high tone again. If we add the reference signal which corresponds to the nominal eye profile, then we can hear the interference between two signals, the nominal one and the distorted one. At normal musical ability the operator can monitor the profile transformation in the course of surgeon operation. Thus we may conclude that the measurements accomplished by the confocal meso-optical keratometer are the direct ones in contrast to the traditional optical keratometer which needs the reconstruction stage to solve the inverse problem.

4. CONFOCAL MESOPTICAL PROFILOMER

The confocal meso-optical keratometer described in § 3 offers important advantages: high spatial resolution, high productivity and the absence of the reconstruction stage inherent to the traditional optical keratometer. But there is one shortage: the profile of the object must be smooth. Meanwhile in the mechanical engineering the profile of the object can contain sudden changes and kinks. These features of the object profile can induce the potential ambiguities. To explain this point let us consider the structure of the longitudinal interference produced by two coaxial wave fronts (Fig.5). The period A of this interference picture is constant.

Now let us consider the principal scheme of the confocal meso-optical profilometer which generates

the interference picture with varying period A . The difference between this device (Fig.6) and the confocal meso-optical keratometer shown in Fig.2 consists in the external (or internal) part of the meso-optical mirror 3. In the device in Fig.6 the generator of this part is the segment of the ellipse with the first focus in the point where the imaginary image of the point light source is formed by the external (or internal) part of the meso-optical mirror 3 and with the second focus in the point which is equally removed from the ellipse segment and from the illuminated region.

Fig.5. The structure of the longitudinal interference picture produced by two coaxial conical wave fronts with angle α between two wave vectors.

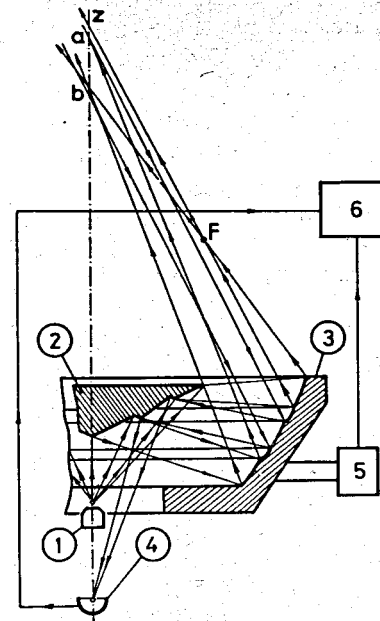


Fig.6. The confocal meso-optical profilometer: 1 - point light source, 2 - concave three element conical mirror, 3 - concave three element meso-optical mirror with generator of the external part in the form of the ellipse segment, 4 - point photodetector, 5 - moving stage with position encoder, 6 - computer memory block.

the interference picture with varying period A . The difference between this device (Fig.6) and the confocal meso-optical keratometer shown in Fig.2 consists in the external (or internal) part of the meso-optical mirror 3. In the device in Fig.6 the generator of this part is the segment of the ellipse with the first focus in the point where the imaginary image of the point light source is formed by the external (or internal) part of the meso-optical mirror 3 and with the second focus in the point which is equally removed from the ellipse segment and from the illuminated region.

The angle between the wave vectors of the interfering conical wave fronts is changing along z -axis, and the period A of the light modulation is varying along z -axis (Fig.7). Here we can use the term from radar^{10,11} where this modulation picture is referred to as "chirp modulation". Thus the confocal meso-optical profilometer shown in Fig.6 generates the chirp-modulated interference

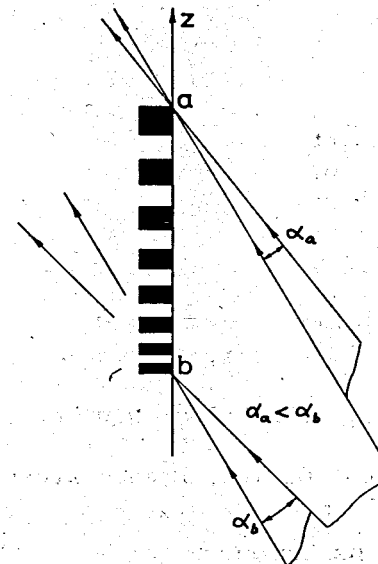


Fig.7. The structure of the longitudinal interference produced in the confocal meso-optical profilometer. The angle α between two wave vectors is a varying function of z -coordinate.

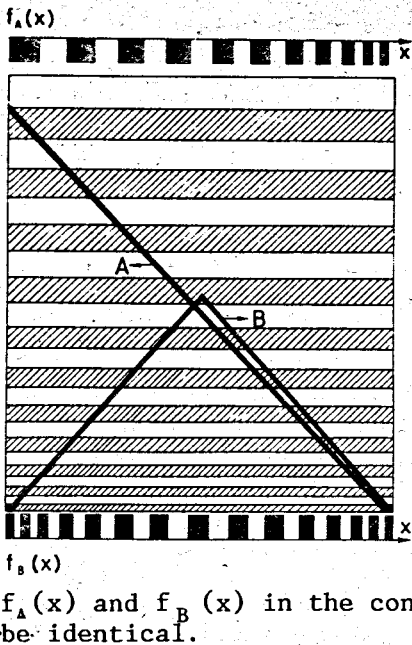


Fig.8. The profiles of two objects A and B and the corresponding output signals: $f_A(x)$ (on the top) and $f_B(x)$ (on the bottom).

picture. In the corresponding two-coordinate grid the period along z-coordinate is changing from $13 \mu\text{m}$ to $18 \mu\text{m}$ thus canceling the ambiguities in the interpretation of the initial photosignals. In Fig.8 there are presented the profiles of two objects A and B. The output signals $f_A(x)$ (on the top) and $f_B(x)$ (on the bottom) are as different as different two profiles A and B. It is evident that the corresponding signals $f_A(x)$ and $f_B(x)$ in the confocal mesoptical keratometer will be identical.

REFERENCES

1. Soroko L.M. - Communication of the JINR, E13-90-592, Dubna, 1990.
2. Soroko L.M. - Communication of the JINR, E13-90-593, Dubna, 1990.
3. Kivaev A.A. - In: Symposium USSR-France, 1980, Midmedprom i Minzdrav USSR, Moscow, p.192.
4. Purjaev D.T. - USSR Patent, No. 1.292.727, Bull. No.8, 1987, p.13.
5. Purjaev D.T. - USSR Patent, No.1.337.042, Bull. No.34, 1987, p.20.
6. Kivaev A.A., Ososkov G.A., Elkind S.A. - Communication of the JINR, 5-84-509, Dubna, 1984.
7. Wilson T. - Appl. Opt., 1981, 20, 3238.
8. Wilson T., Sheppard C.J.R. - Theory and Practice of Scanning Optical Microscope, Academic Press, London, 1984.
9. Soroko L.M. - Progress in Optics, ed. E.Wolf, Elsevier, Amsterdam, 1989, 27, 109.
10. Mertz L. - Transformation in Optics, John Wiley, New York, 1965.
11. Soroko L.M. - Holography and Coherent Optics, Plenum Press, New York, 1980.

Received by Publishing Department
on December 28, 1990.